Macromol. Symp. ***142,*** *43–59 (1999)*

Synthesis and Solution Properties of Rodlike Polyelectrolytes

Matthias Wittemann, Steffen Kelch, Jürgen Blaul, Peter Hickl, Birgit Guilleaume,
Gisela Brodowski, Andreas Horvath, Matthias Ballauff*, Matthias Rehahn*
Polymer Institute, University of Karlsruhe, Kaiserstrasse 12, D-76128 Karlsruhe,
Germany

SUMMARY: The synthesis and the solution behavior of rigid, rodlike cationic polyelectrolytes having (*i*) poly(*p*-phenylene) backbones and (*ii*) main chains composed of 4,4"-bis(2,2':6',2"-terpyridine)2',5'-dihexyl-*p*-terphenyl moieties and ruthenium(II) centers are presented. All these polymers are shown to have a homogeneous constitution and degrees of polymerization of up to $P_n \approx 70$. Their solution properties were analyzed using viscosimetry, small-angle X-ray scattering (SAXS) and osmometry. Pronounced polyelectrolyte effects were found in salt-free solutions using viscosimetry. Small-angle X-ray scattering demonstrated directly the strong correlation of the counterions and the macroions. The osmotic coefficients measured in salt-free solution as function of polyelectrolyte concentration were found to be lower than predicted by the cell model.

Introduction

The understanding of flexible polyelectrolytes in dilute solutions of low ionic strength still presents a considerable challenge in macromolecular science, despite of many decades of research1-4). This is due to the long-range nature of the coulombic forces between the charged macromolecules. In the case of flexible polyelectrolytes, a decrease of the ionic strength may lead to an expansion of the coils due to strong intramolecular forces as well as to stronger intermolecular electrostatic interactions. Conformationally rigid, rodlike polyelectrolytes, on the other hand, remain in their extended chain conformation regardless of the ionic strength of the system. Because conformative and excluded volume effects are ruled out here, only the intermolecular coulombic interactions determine the solution properties of these polymers.

Based on these considerations, a number of studies have been performed using naturally occurring rodlike helical polyelectrolyte systems such as DNA or xanthane5). However, at very low ionic strengths and at elevated temperatures the helical conformation and thus the rodlike shape are lost. Moreover, systematic variation of the charge density, *i.e.* the number of ionic groups per unit length, is not possible with the aid of these biopolymers. Therefore, the development of well-defined synthetic rodlike polyelectrolytes is necessary to analyze

CCC 1022-1360/99/$ 17.50+.50/0

quantitatively intermolecular interactions, counterion condensation, and structure formation in solution depending on ionic strength, temperature, and polyelectrolyte concentration.

First synthetic rodlike polyelectrolytes were published in the early eighties(6,7) which based on poly(1,4-phenylenebenzobisoxazoles) and poly(1,4-phenylenebenzobisthiazoles). In the recent decade, we(8-12) and others(13,14) developed various efficient precursor routes to synthetic rodlike poly(*p*-phenylene) (PPP) polyelectrolytes which take advantage of both the concept of solubilizing side chains(15,16) and the efficient Pd-catalyzed aryl-aryl coupling reaction(17-19). This progress was rendered possible mainly by (*i*) the high tolerance of the Pd-catalyzed polycondensation reactions toward functional groups in the starting materials and (*ii*) the outstanding thermal and chemical stability of the PPP backbone which allows transformation of the uncharged precursor PPPs into polyelectrolytes by a variety of organic reactions. By these precursor routes, high-molecular-weight carboxylated and sulfonated PPP polyelectrolytes with homogeneous constitution and well-known degrees of polymerization (P_n) have been prepared first (see, for example: Scheme 2, structures **7** and **8**). The polymers thus available combine exceptional hydrolytic, thermal and chemical stability with a high charge density of up to two ionic groups per *p*-phenylene repeating unit. Unfortunately, however, all these anionic PPP polyelectrolytes certainly dissolved in polar organic solvents or mixtures thereof with water but were insoluble in water or aqueous bases. Therefore, cationic PPP polyelectrolytes have been prepared as well which were expected to be much better soluble in water. The results thus obtained will be described in the first part of the present paper. Moreover, for comparison purposes, we additionally prepared rodlike cationic ruthenium(II) coordination polyelectrolytes. Hence, the second part of this paper presents a description of the synthetic route developed for the preparation of these readily soluble and constitutionally well-defined transition-metal containing macromolecules as well as of their properties in solution.

Synthesis of PPP polyelectrolytes

A series of uncharged precursor PPPs **3** - **5** has been prepared according to Scheme 1, bearing phenoxy substituents at the ends of either some or even all of their solubilizing *n*-hexyl side chains(10,11,20). These phenoxy groups represent ideal precursor functionalities because they are inert under the conditions of the Pd-catalyzed polycondensation but can be activated easily and completely for the subsequent introduction of the desired charged groups via macromolecular substitution routes. The precursor strategy thus used for the preparation of the cationic PPP polyelectrolytes has moreover the distinct advantage that the uncharged precursors **3** - **5** can be fully characterized without being affected by the well-known problems associated with charged macromolecules. NMR spectroscopy proved their defect-free constitution, and number-average degrees of polymerization of up to $P_n = 70$ were determined reliably using membrane osmometry for all these precursors. The persistence length of the PPP backbone was estimated[21)] by Bohdanecky's method[22)] to be 22 nm. This is in good agreement with the results from a recent computer simulation[23)] but considerably higher than the value of 13 nm deduced from a similar PPP recently by Vanhee et al.[14)] Despite of this discrepancy, it seems to be justified to regard the PPP derivatives under consideration here (contour lengths of 10 to 40 nm) as rodlike entities.

Scheme 1

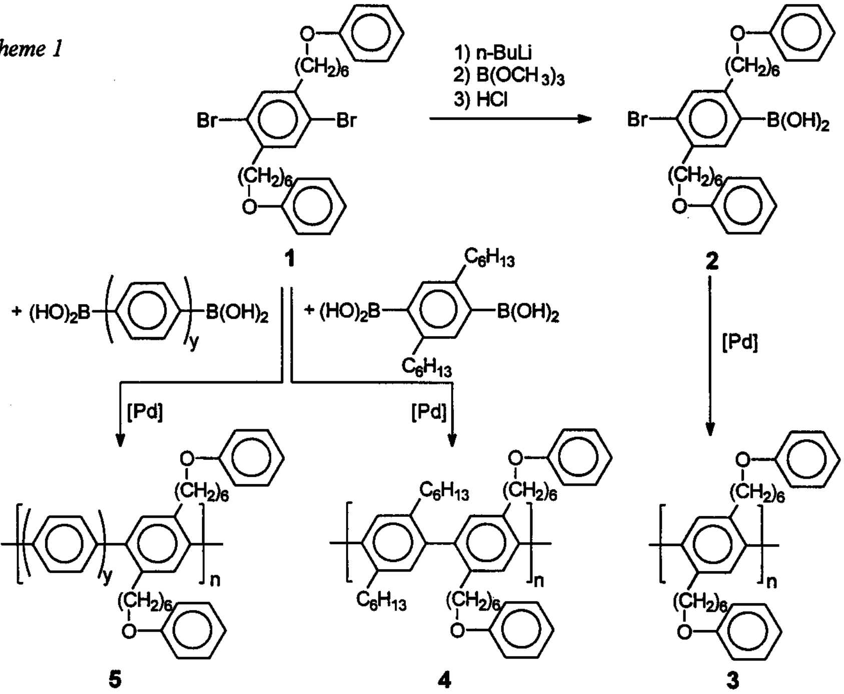

After their full characterization, the precursors **3** - **5** were converted into cationic PPP polyelectrolytes via the route shown in Scheme 2 for PPP derivative **3**: Firstly, the phenoxy groups were cleaved off quantitatively using trimethyliodosilane. In the second step, the cationic ammonium or pyridinium groups were introduced via quaternization of the 6-iodohexyl substituted precursor PPPs with tertiary amines such as triethylamine or pyridine. All the thus obtained PPP polyelectrolytes proved to be readily soluble in, for example, acetonitrile and dimethylacetamide, some of them even in pure water. Their ^1H and ^{13}C NMR spectra showed full conversion under the used conditions: The quaternization resulted in the complete disappearance of the iodomethylene absorptions, and all new signals in the NMR spectra were in full agreement with the molecular structures of the desired polyelectrolytes. Side reactions such as elimination or cross-linking processes were thus excluded for sure within the scope of accuracy of the NMR method. Moreover, no fractionation was admitted during the workup. Therefore, identical values of P_n can be assumed for the polyelectrolytes thus obtained as determined in advance for their precursors.

Scheme 2

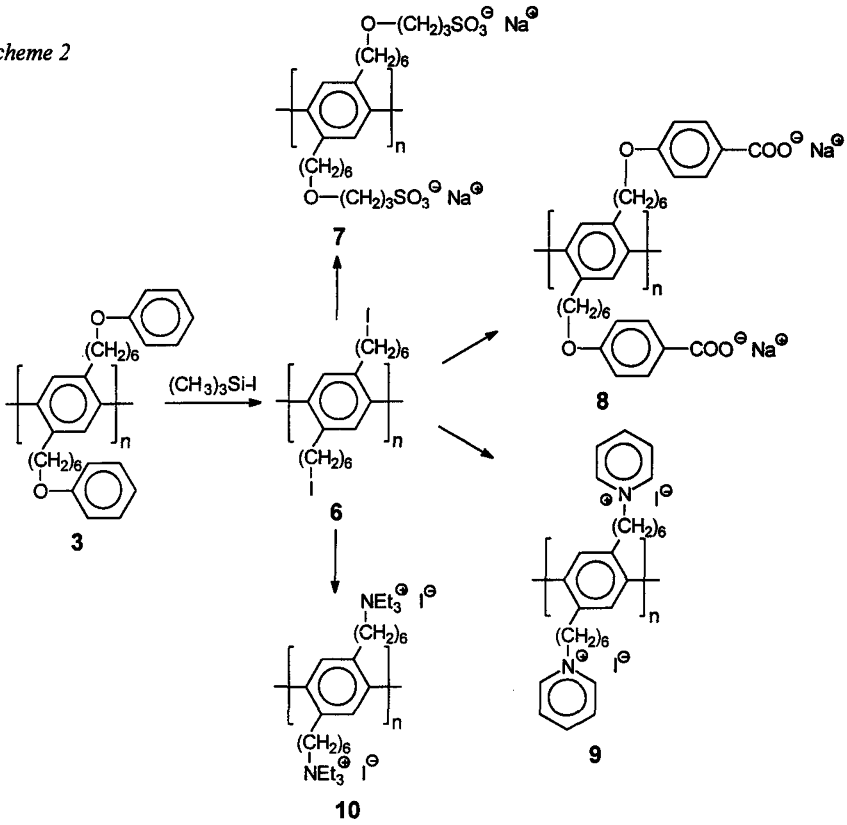

In addition to the readily water-soluble PPP polyelectrolytes such as **9** and **10** having two charged groups per phenylene repeating unit, we were also interested in making available further PPP derivatives having an even higher charge density. Therefore, an efficient two-step quaternization route was developed, leading to PPP polyelectrolytes **12** with as many as four tetraalkyl ammonium groups per *p*-phenylene repeating unit, *i.e.*, every 4.5 ångstrøms. For this purpose, precursor PPP **6** was first reacted with an approximately fourhundredfold molar excess of tetramethylethylenediamine (TMEDA) in a solvent mixture of chloroform and acetonitrile (Scheme 3). The large excess of TMEDA used in the synthesis of **11** is essential in order to suppress quaternization of both TMEDA nitrogen atoms in this first step which would lead to structural irregularities and crosslinks. After workup and purification by ultrafiltration, the remaining TMEDA amino groups of **11** were quaternized. For this purpose, the brownish, foamy material **11** was redissolved in dimethylsulfoxide and heated in the presence of a slight excess of iodoethane. The progress of the conversion was monitored using NMR spectroscopy. A prolonged reaction time and forced conditions were found to be necessary here to achieve complete conversion. The resulting polyelectrolyte solutions were again purified by ultrafiltration.

Scheme 3

6

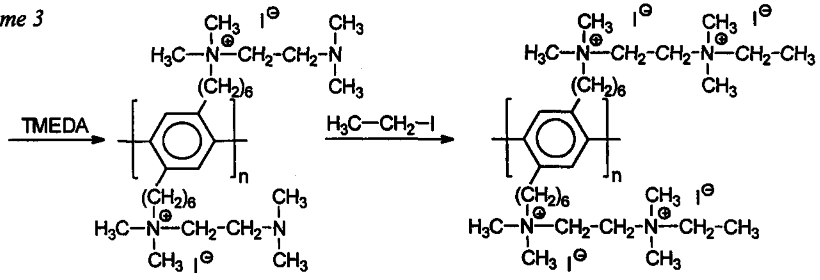

11 **12**

The homogeneous constitution of intermediate **11** as well as of the doubly quaternized polyelectrolyte **12** was proved using high-resolution NMR spectroscopy. Moreover, because no evidence of chain degradation was found and no polymeric material passed through the membranes used for ultrafiltration, the obtained polyelectrolytes **11** and **12** have the same degrees of polycondensation as the precursor PPPs **3** and **6** used for their preparation, *i.e.* PPP polyelectrolytes **11** and **12** became available with values of P_n of 20 - 70 (M_n = 15 000 - 50 000 $g{\cdot}mol^{-1}$).

Finally, we would like to emphasize that the PPP polyelectrolytes **9** - **12** are excellently soluble in water, despite their highly hydrophobic skeleton. This is presumably due to the fact that these macromolecules represent cylinders of an average length of l_c = 90 - 300 Å and a diameter of $d_c \approx$ 10 Å whose hydrocarbon core is covered by the highly polar and thus hydrophilic shell of tetraalkylammonium groups.

Solution properties of PPP polyelectrolytes

Polymer **10** was chosen for all subsequent studies because it is easily available in the gram scale and excellently soluble in water. Moreover, because it bears two charged groups per repeat unit at the ends of the hydrophobic *n*-hexyl side chains, this material was expected to have solution properties almost undisturbed by the hydrophobic moieties of the repeating units. The P_n of polymer **10** discussed here was 40.

a) Viscosimetry

Figure 1 shows the plot of the reduced specific viscosities as function of polymer concentration (Huggins plot) of PPP polyelectrolyte **10** in pure water (■), and in salt-containing solutions having (□) 0.010, (▽) 0.025, and (▲) 0.050 g · L^{-1} of $NEt_4^+I^-$ as added salt.

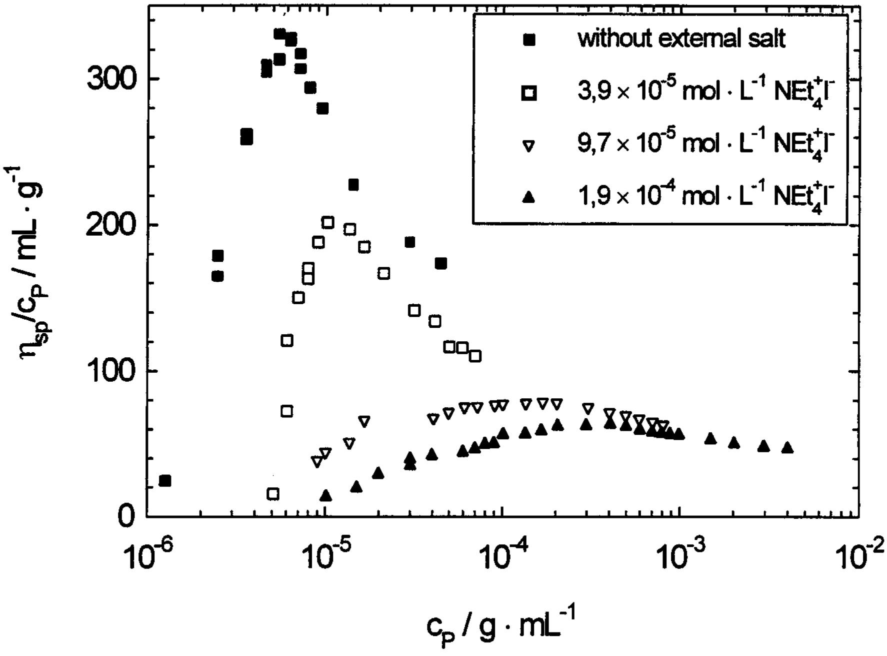

Fig. 1: Huggins plots of PPP polyelectrolyte **10** in pure water (■), and in salt-containing solutions having (□) 0.010, (▽) 0.025, and (▲) 0.050 g · L^{-1} of $NEt_4^+I^-$.

Without added salt, or at very low concentration of external salt, distinct maxima are found in the Huggins plots of polyelectrolyte **10** which became less and less pronounced with increasing ionic strength. Moreover, the maxima shift from $c_P \approx 5 \times 10^{-6}$ g · mL^{-1} (without added salt) to higher polymer concentrations (such as $c_P \approx 4 \times 10^{-4}$ g · mL^{-1} for 1.9×10^{-4} *M* aqueous $NEt_4^+I^-$). If the measurements were finally performed at very high concentration of added salt, *i.e.* in 0.01 *M* aqueous $NEt_4^+I^-$, the data could be fitted by a straight line (not shown). Here, the intrinsic viscosity of the PPP polyelectrolyte **10** under investigation was found to be [η] = 29 mL · g^{-1}. Due to the high ionic strength, the intermolecular coulombic interactions of the polymer chains are strongly screened out in this latter solution. The intrinsic viscosity of **10** obtained under these conditions is in excellent agreement with the value of [η] measured for its uncharged precursor PPP **3** ([η] = 31 mL · g^{-1}, measured in 1,1,2,2-tetrachloroethane at 35 °C). This result further supports our assumption that changes of the values of P_n during the conversion of the precursor PPPs into the PPP polyelectrolytes are negligible.

The observed hydrodynamic behavior of polymer **10** is in qualitative agreement with recent findings on flexible polyelectrolytes. However, there are marked quantitative differences. For example, the maxima in the Huggins plots of the rodlike PPP polyelectrolytes appear at considerably lower polymer concentrations — approximately one order of magnitude — than the maxima appear in the case of coiled polyelectrolytes of similar chain lengths when measurements are performed in solutions of comparable ionic strength. Moreover, the observed polyelectrolyte effect is much more pronounced in the case of the rodlike PPP polyelectrolytes than in the case of coiled polyelectrolytes of similar chain length and charge density. A detailled analysis of these findings and their quantitative description by means of theoretical models is under way.

b) SAXS investigations

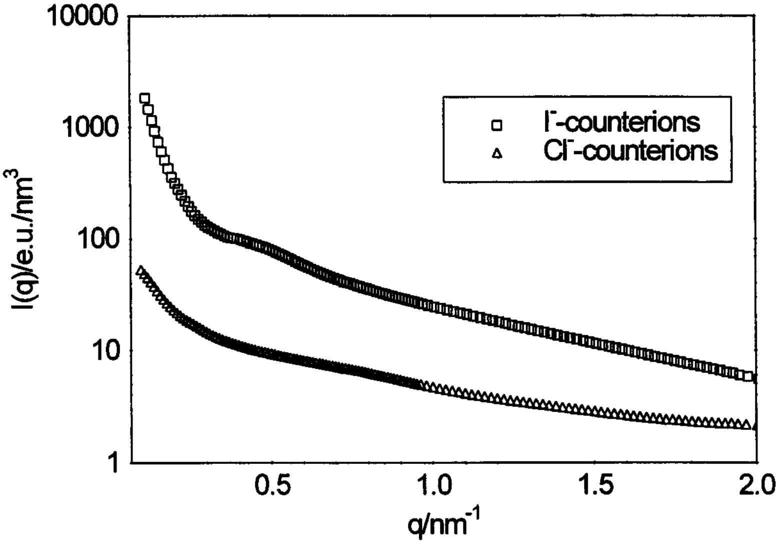

Fig. 2: Absolute SAXS-intensities measured from solutions of polyelectrolyte **10** in aqueous solution at a concentration of 10 g · L^{-1}. Two counterions have been used: Iodine (squares) counterions having a high contrast towards water and chlorine (triangles) counterions which are nearly matched by water.

To assess the correlations of the counterions and the macroions in more detail, the PPP-polyelectrolyte **10** has been studied in solution using small-angle X-rays scattering (SAXS). By changing the counterions from Cl^- to I^- the contrast can be changed quite drastically: While the electron density of Cl^- ions is nearby matched by water, I^- ions exhibit a strong contrast in aqueous solution. Hence, if I^- counterions are used, their correlation with the macroion should be easily visible. In case of Cl^- counterions, on the other hand, the measured scattering intensity is dominated by the macroions.

SAXS measurements in solution were performed as described recently[24]. Details of measurements and data evaluation will be given elsewhere[25]. Fig. 2 displays the desmeared SAXS intensities of the polyelectrolyte **10** with I^- counterions (squares) and with Cl^- counterions. The marked difference between both sets of data is immediately obvious: The scattering intensities measured in case of I^- counterions are much higher. This finding points immediately to the strong correlation of the counterions and the macroion: If the I^- counterions were dispersed at random in the solution, their contribution to the measured scattering intensity would be small. If, however, most of the counterions are located in the immediate vicinity of the macoion ("counterion condensation"), strong spatial inhomogeneity of the excess electron density would follow, leading to the observed strong scattering.

Both sets of data can be evaluated to yield quantitative information on the radial distribution of counterions. Hence, these measurements may serve for a quantitative check of current models of rodlike polyelectrolytes as *e.g.* the cell model. A study of this problem by SAXS is under way[25].

c) Osmotic measurements

The osmotic coefficient of salt-free polyelectrolyte solutions is a classical subject of polymer research[26]. As in case of the above SAXS data, the resulting data can immediately be compared with the cell model of rodlike polyelectrolytes[27,28]. In the frame of the cell model, the polyelectrolyte is characterized by the charge parameter[26-28], ξ, which is defined through the ratio of the Bjerrum length, λ_B, to the contour distance per unit charge, b:

$$\xi = \frac{\lambda_B}{b} \qquad (1)$$

with λ_B being defined through

$$\lambda_B = \frac{e^2}{4\pi\varepsilon_0 \varepsilon k_B T} \qquad (2)$$

where e is unit charge, ε the dielectric constant of the medium and ε_0, k_B and T have their usual meanings. Within the frame of the Manning theory[29,30] a certain fraction of the counterions is bound to the macroion if ξ exceeds unity. The rest of the counterions remains "free" and forms a Debye-Hückel cloud around the macroion.

For solutions without added salt, the fraction of free counterions may be expressed through the osmotic coefficient ϕ. This quantity is defined by the ratio of the measured osmotic pressure Π and the ideal osmotic pressure Π_{id} calculated for a solution of free counterions

$$\phi = \frac{\Pi}{\Pi_{id}} \qquad (3)$$

In this case, the Manning theory arrives for $\xi > 1$ at a particularly simple result for the osmotic coefficient at infinite dilution, namely[29,30)]

$$\phi = \frac{1}{2\xi} \qquad (4)$$

In the case to be discussed here, *i.e.* solutions of the polyelectrolyte without added salt, the PB-cell model can be solved exactly[31,32)] to yield the osmotic coefficient for finite concentrations of the polyelectrolyte as well:

$$\phi = \frac{1-\beta^2}{2\xi} \qquad (5)$$

Here, β is an integration constant which is related to the concentration of the polyelectrolyte in solution and the radius of the macroion[31,27,28)]. Hence, given these quantities ϕ may be calculated from the cell model[31)] without resort to adjustable parameters. Data of the osmotic coefficient may therefore serve as a sensitive test of the cell model of rigid-rod polyelectrolytes.

Fig. 3 displays the osmotic coefficient measured on a salt-free solution of the PPP polyelectrolyte **10** in water at 40°C. Details of the measurements will be given elsewhere[33)]. The charge parameter has been determined from structural data of the polyelectrolyte **10**. As it turned out, the osmotic coefficient ϕ is not very sensitive towards the diameter a of the macroion which presents the only adjustable parameter for the comparison of theory and experiment. Here we chose a = 0.5 nm which seems to be a reasonable value for the rodlike polyelectrolyte under consideration. Hence, the comparison between the cell model (eq.(5)) and the measured data proceeds virtually parameter-free.

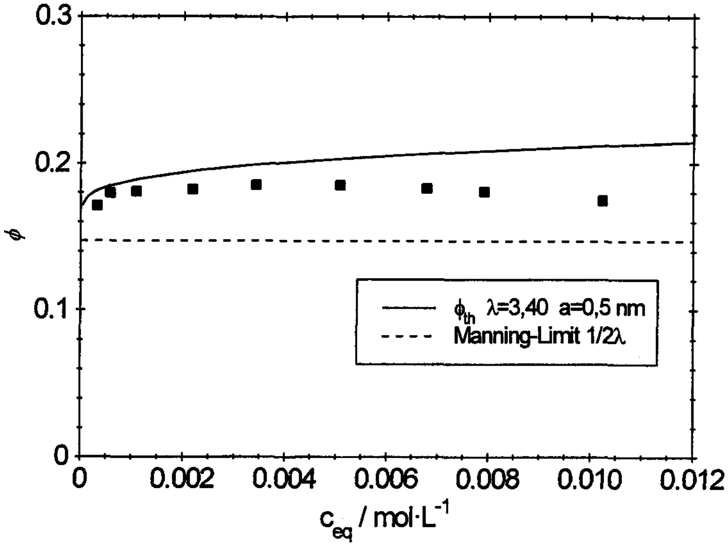

Fig. 3: Osmotic coefficient (see eq.(3)) of salt-free solutions of the polyelectrolyte **10** (squares) together with the theoretical predictions of the cell model[31)] (solid line, eq.(5)) and of the Manning theory[29,30)] (dashed line; eq.(4)). From ref.[33)]

It is evident that the experimental data are located between the prediction of the cell model given by eq.(5) and the Manning limit (eq.(4)). The cell model overestimates ϕ considerably, in particular when going to higher polymer concentrations. Similar findings have been reported from solutions of flexible polyeletrolytes[26)]. Here agreement of theory and experiment was achieved by adjusting the length per unit charge, *i.e.*, by using the charge parameter ξ as an adjustable parameter. In the case of the stiff-chain polyelectrolyte **10** this procedure is no longer possible. The present comparison therefore demonstrates that the theory of the osmotic coefficient is in need of revision. This finding is in agreement with recent theoretical work[34)].

The osmotic coefficient furnished by the Manning theory (dashed line in fig. 3) must be regarded as a limiting value to be found at exceedingly low concentration being not accessible experimentally[34)]. Agreement of the experimental data with ϕ derived from eq.(4) cannot be expected. A more detailed discussion of the osmotic coefficient of the rodlike polyelectrolytes **10** is under way[33)].

Synthesis of stiff-chain ruthenium(II) coordination polyelectrolytes

Soluble, constitutionally well-defined ruthenium(II) coordination polymers are of actual interest because of their electronic, photooptical, magnetic and catalytic properties[35-42]. Moreover, they represent important model systems for the profound analysis of polyelectrolyte behavior in dilute solution. Therefore, we developed efficient synthetic routes leading to conformationally rigid, high-molecular-weight coordination polyelectrolytes **13a-d** and **16**[43-46]. While polymers **13** form random coils and thus are not considered in detail here, polymers **16** are rodlike in shape. Their preparation was possible via the conversion of 4,4"-bis(2,2':6',2"-terpyridine)-2',5'-dihexyl-*p*-terphenyl **14** with an activated ruthenium(III) species such as **15**[47,48] in a solvent mixture of DMA and 1-butanol (Scheme 4). Because of the flexible *n*-hexyl side chains, the dark-red, fibrous rodlike polymers **16** proved to be readily soluble in various organic solvents such as DMA or DMSO, and their constitution could be verified using ^1H and ^{13}C NMR spectroscopy: All observed absorptions clearly corresponded to the inner-chain repeating units of **16**, and no absorptions could be found pointing towards defect structures or end-groups. Moreover, by means of model investigations we could prove that these latter absorptions are not only covered by the broad signals of the repeating units but are really absent. Hence, because end-groups absorptions obviously have intensities below the limits of accuracy of the NMR method for polymers **16** prepared from an exact 1:1 stoichiometry of comonomers **14** and **15**, and because formation of cyclic oligomers can be excluded due to the rodlike shape of **16**, we concluded that really high-molecular-weight polymers were produced: Considering the limits of the NMR method, we estimated average degrees of polymerisation of $P_{n(NMR)} \geq 30$ ($M_n \geq 30\ 000\ g \cdot mol^{-1}$) for the best products synthesized so far.

Solution properties of ruthenium(II) coordination polyelectrolytes

The hydrodynamic behavior of coordination polyelectrolytes **16** was analyzed both in salt-free and in salt-containing DMA solutions using viscosimetry. In a first series of experiments, polyelectrolytes **16** were studied in 0.02 M NH_4PF_6 / DMA. Under these conditions, the intermolecular Coulomb interactions between the charged macromolecules are screened out, and evaluation of the measured data is possible according to the procedures usually applied for uncharged polymers. Fig. 4 displays the Huggins plots of (**A**) a high-molecular-weight sample of **16** ($P_{n,NMR} \geq 30$), of (**B**) a low-molecular-weight sample of **16** ($P_{n,NMR} < 10$), and — for comparison purposes — of (**C**) a high-molecular-weight sample of the coiled ruthenium(II) coordination polymer **13d** ($P_{n,NMR} \geq 30$) bearing adamantylmethylene side groups.

Scheme 4

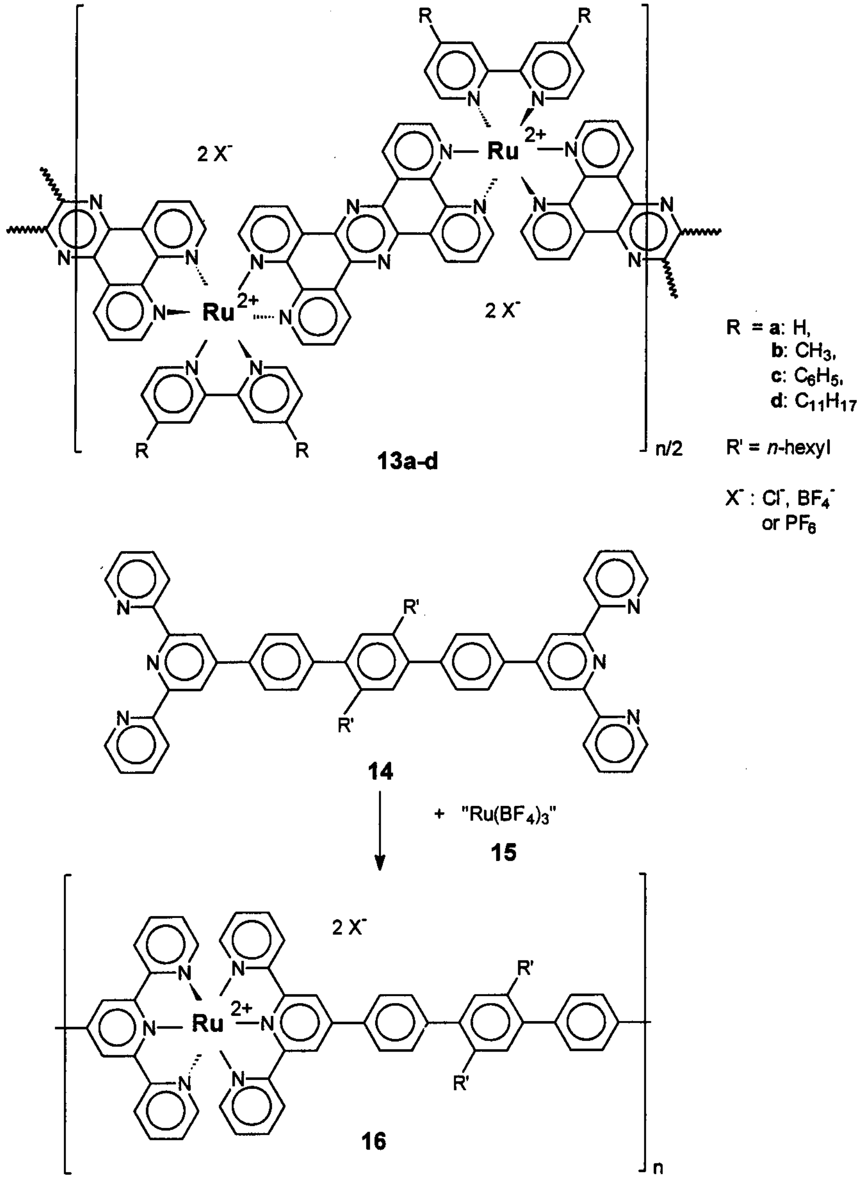
2 X⁻
Ru 2+
Ru 2+
2 X⁻
R
R
R
R
13a-d
n/2
R = a: H,
b: CH3,
c: C6H5,
d: C11H17
R' = n-hexyl
X⁻ : Cl⁻, BF4⁻
or PF6
R'
R'
14
+ "Ru(BF4)3"
15
2 X⁻
Ru 2+
R'
R'
16
n

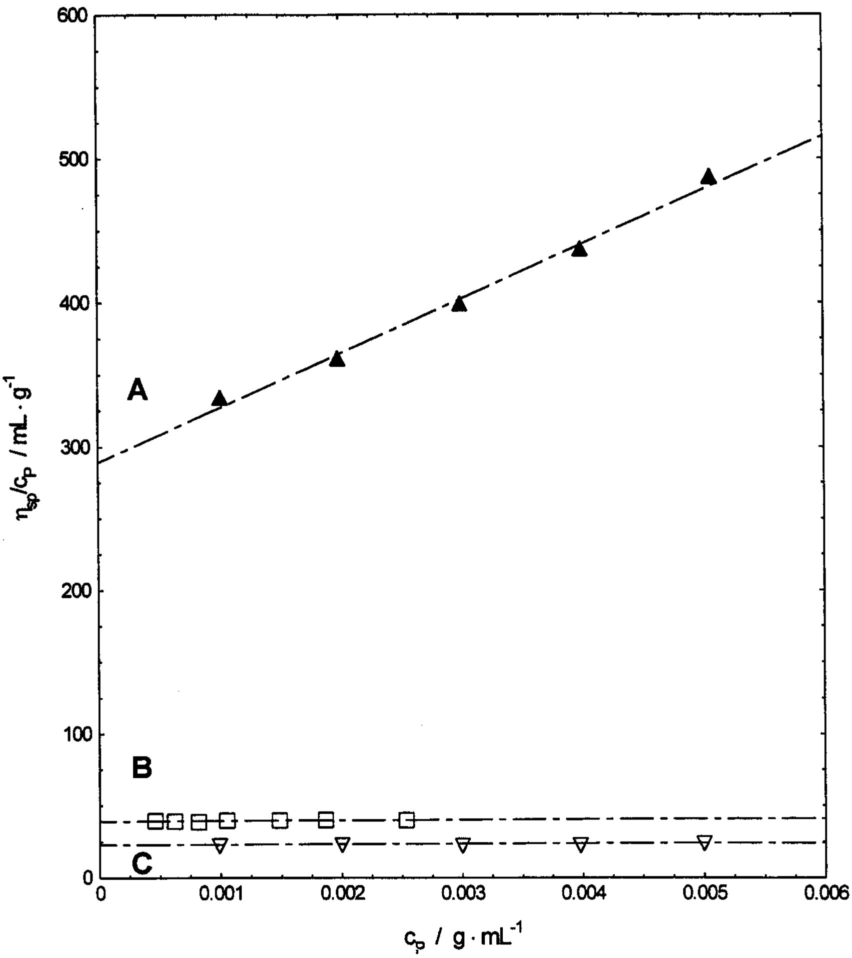

Fig. 4: Huggins plots (**A**) of a high-molecular-weight sample of **16** ($P_{n,NMR} \geq 30$), (**B**) of a low-molecular-weight sample of **16** ($P_{n,NMR} < 10$), and (**C**) of a high-molecular-weight sample of the coiled ruthenium(II) coordination polymer **13d** ($P_{n,NMR} \geq 30$) bearing adamantylmethylene side groups, recorded in 0.02 M NH_4PF_6 / DMA solution.

In all three cases, linear extrapolation of the values of η_{sp}/c_P is possible to $c_P = 0$ g · mL^{-1}. An intrinsic viscosity of $[\eta] \approx 300$ mL · g^{-1} is determined for the high-molecular-weight sample of polymer **16**. This value is approx. one order of magnitude higher than the values of $[\eta]$ determined for the rodlike oligomer **16** ($[\eta] \approx 40$ mL · g^{-1}) and for the high-molecular-weight but randomly coiled ruthenium(II) coordination polymer **13d** ($[\eta] \approx 25$ mL · g^{-1}). Moreover, a value of $[\eta] \approx 300$ mL · g^{-1} is not only the highest value ever observed for a ruthenium(II) coordination polymer but is even higher than those found for many other molecular-dispersely soluble, rodlike macromolecules held together by covalent bonds only. Poly(*p*-phenylenes) **17**, for example, have a value of $[\eta] = 207$ mL · g^{-1} when the value of P_n is 37 (osmometry)[21,49)]. For rodlike polyimides **18**, moreover, a value of $[\eta] = 268$ mL · g^{-1} is found for samples having $P_n = 46$ (osmometry) and $P_w = 111$ (static light scattering)[50)]. The polyimide **18**, for example, has an average of 46 repeating units per chain and hence an average chain length of $l_n = 96$ nm (the length of the monomeric unit is $l_u = 2.09$ nm)[50)]. As the intrinsic viscosity of the sample of **18** under consideration is still somewhat lower than that of **16**, it is reasonable to assume that the average chain length of the novel ruthenium(II) coordination polymers **16** is at least similar. That means if polymer **16** has an average chain length of $l_n \approx 100$ nm as well, its P_n is approx. 43 ($l_u = 2.32$ nm).

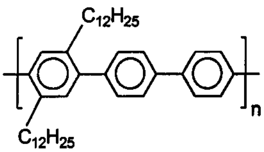

17

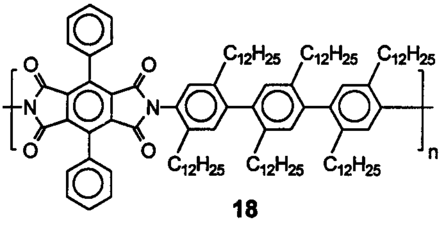

18

This comparison additionally supports the anticipated high molecular weights of coordination polymers **16**. Even if this procedure does not give the exact values of P_n it nevertheless strongly supports the results from NMR spectroscopy. Moreover, it also supports the rodlike shape of **16**: If it had a substantially flexible or even coiled backbone, neither the high values of the intrinsic viscosity nor the tremendeous influence of the chain length on the intrinsic viscosity would be observed.

In a second series of experiments, the hydrodynamic behavior of coordination polyelectrolytes **16** was studied in pure DMA and thus at low ionic strength. Under these conditions, the intermolecular Coulomb interactions between the charged macromolecules are in operation. Fig. 5 displays the Huggins plot of (**A**) a high-molecular-weight sample of **16** ($P_{n,NMR} \geq 30$), of (**B**) a low-molecular-weight sample of **16** ($P_{n,NMR} < 10$), and of (**C**) a high-molecular-weight sample of the coiled polymer **13a** ($P_{n,NMR} \geq 30$). Under salt-free conditions as well, the high-molecular-weight polymer **16** stands out from the other samples: It displays by far the most pronounced polyelectrolyte effect. A maximum of $(\eta_{sp}/c_P)_{max} \approx 2000$ mL · g^{-1} is found for this sample in the Huggins plot at a polymer concentration of $c_P \approx 5\times10^{-6}$ g · mL^{-1}. However, the corresponding maximum is also clearly detectable for the low-molecular-weight rodlike system **16** where a value of $(\eta_{sp}/c_P)_{max} \approx 500$ mL · g^{-1} is reached at approx. the same polymer concentration of $c_P \approx 5\times10^{-6}$ g · mL^{-1}. Finally, as expected, the maximum of the reduced specific viscosity of the high-molecular-weight but randomly coiled reference polymer **13a** is again less pronounced $\{(\eta_{sp}/c_P)_{max} \approx 100$ mL · g$^{-1}\}$. It appears at a polymer concentration of $c_P \approx 9\times10^{-5}$ g · mL^{-1} which is more than one order of magnitude higher than the concentration where the maximum is found for polymers **16**.

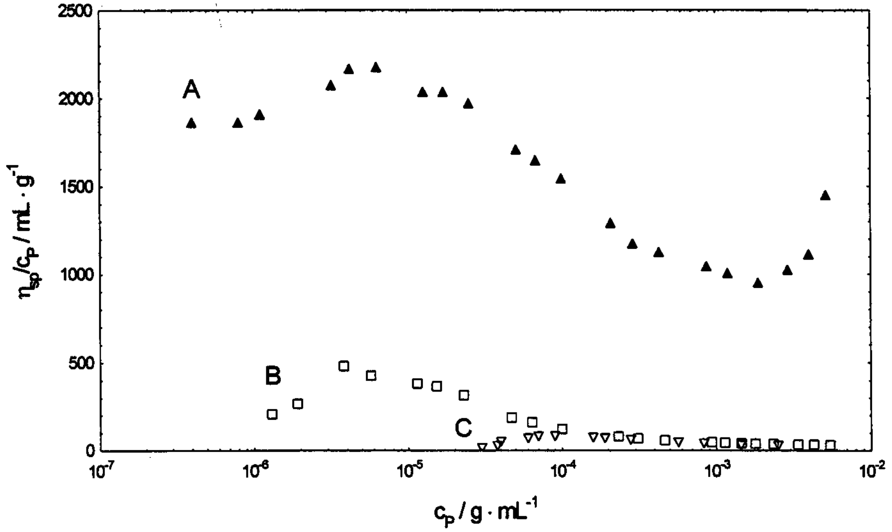

Fig. 5: Huggins plot of (**A**) a high-molecular-weight sample of **16** ($P_{n,NMR} \geq 30$), (**B**) a low-molecular-weight sample of **16** ($P_{n,NMR} < 10$), and (**C**) a high-molecular-weight sample of the coiled polymer **13a** ($P_{n,NMR} \geq 30$), recorded in salt-free DMA solution.

These results highlight the considerable influence of the chain length and in particular of the shape of the macromolecules on their hydrodynamic behavior also in solutions of low ionic strength: Extended chains give rise to much more pronounced polyelectrolyte effects than chains of similar length but coiled conformation. Moreover, while the P_n influences the values of $(\eta_{sp}/c_P)_{max}$ considerably in the case of the rodlike polyelectrolytes **16**, this effect is much less pronounced in the case of the coiled systems **13**.

Finally, comparison of the hydrodynamic behavior of the low-molecular-weight polymer **16** with that of the rodlike PPP polyelectrolyte **10** described above might be instructive. In the latter case, a value of $(\eta_{sp}/c_P)_{max} \approx 350$ mL·g^{-1} is found in salt-free aqueous solution at $c_P \approx 5\times10^{-6}$ g·mL^{-1} in the Huggins plot of a sample **10** having a P_n of 40 (osmometry). This value of P_n corresponds to an average chain length of $l_n \approx 17.6$ nm ($l_u = 0.44$ nm). The low-molecular-weight polymer **16**, on the other hand, which has a $P_{n,NMR} < 10$ and thus an average length of $l_n < 23.2$ nm, shows a maximum in the Huggins plot of $(\eta_{sp}/c_P)_{max} \approx 500$ mL·g^{-1} (Fig. 5, curve **B**). At first glance, these two results fit fairly well. However, prior to a final assessment and more extensive conclusions, the influence of the solvent and of the shear gradient on the observed quantities must be investigated in more detail.

Conclusions

We described the synthesis and the behavior in solution of rigid, rodlike cationic polyelectrolytes having (*i*) poly(*p*-phenylene) backbones and (*ii*) main chains composed of 4,4"-bis(2,2':6',2"-terpyridine)2',5'-dihexyl-*p*-terphenyl moieties and ruthenium(II) centers. All these polymers are shown to have a homogeneous constitution and degrees of polymerization of up to $P_n \approx 70$. Their solution properties could be analyzed using viscosimetry, small-angle X-ray scattering (SAXS) and osmometry. Pronounced polyelectrolyte effects were found in salt-free solutions using viscosimetry. Small-angle X-ray scattering demonstrated directly the strong correlation of the counterions and the macroions. The osmotic coefficients measured in salt-free solution as function of polyelectrolyte concentration were found to be lower than predicted by the cell model.

References

1) S. Förster, M. Schmidt, *Adv. Polym. Sci.* **120**, 51 (1995)
2) K. S. Schmitz, *Macroions in solution and colloid suspension*, VCH Publishers: New York, 1993
3) S. Förster, M. Schmidt, M. Antonietti, *Polymer* **31**, 781 (1990)
4) M. J. MacCallum, C. A. Vincent, *Polymer Electrolyte Reviews*, Elsevier: London, 1987
5) K. Kassapidou, W. Jesse, M. E. Kuil, A. Lapp, S. Egelhaaf, J. R. C. van der Maarel, *Macromolecules* **30**, 2671 (1997)
6) C. C. Lee, S.-G. Chu, G. C. Berry, *J. Polym. Sci.: Polym. Phys. Ed.* **21**, 1573 (1983)
7) P. Metzger Cotts, G. C. Berry, *J. Polym. Sci.: Polym. Phys. Ed.* **21**, 1255 (1983)
8) I. U. Rau, M. Rehahn, *Makromol. Chem. Phys.* **194**, 2225 (1993)
9) I. U. Rau, M. Rehahn, *Polymer* **34**, 2889 (1993)
10) I. U. Rau, M. Rehahn, *Acta Polymerica* **45**, 3 (1994)
11) G. Brodowski, A. Horvath, M. Ballauff, M. Rehahn, *Macromolecules* **29**, 6962 (1996)
12) M. Wittemann, M. Rehahn, *J. Chem. Soc., Chem. Commun.* 623 (1998)
13) R. Rulkens, M. Schulze, G. Wegner, *Macromol. Rapid Commun.* **15**, 669 (1994)
14) S. Vanhee, R. Rulkens, U. Lehmann, C. Rosenauer, M. Schulze, W. Köhler, G. Wegner, *Macromolecules* **29**, 5136 (1996)
15) M. Ballauff, *Mater. Sci. Tech.* **12**, 213 (1993)
16) M. Ballauff, *Angew. Chem.* **101**, 261 (1989)
17) M. Rehahn, A.-D. Schlüter, G. Wegner, W. J. Feast, *Polymer* **30**, 1060 (1989)
18) M. Rehahn, A.-D. Schlüter, G. Wegner, *Makromol. Chem. Phys.* **191**, 1991 (1990)
19) A.-D. Schlüter, G. Wegner, *Acta Polym.* **44**, 59 (1993)

20) G. Brodowski, *PhD thesis*, Karlsruhe, Germany, 1999

21) P. Galda, *PhD thesis*, Karlsruhe, Germany, 1994

22) M. Bohdanecky, *Macromolecules* **16**, 1483 (1983)

23) B. L. Farmer, B. R. Chapman, D. S. Dudis, W. W. Adams, *Polymer* **34**, 1588 (1993)

24) P. Hickl, M. Ballauff, U. Scherf, K. Müllen, P. Lindner, *Macromolecules*, **30**, 273 (1997)

25) B. Guilleaume, M. Ballauff, in preparation

26) M. Mandel, *Polyelectrolytes.* In *Encyclopedia of Polymer Science and Engineering*, 2nd edition, F. H. Mark, N. M. Bikales, C. G. Overberger, G. Menges, Eds., Wiley, New York, 1988, Vol. 11, p. 739

27) A. Katchalsky, *Pure Appl. Chem.* **26**, 327 (1971) and further references given there

28) M. Mandel, *J. Phys. Chem.* **96**, 3934 (1992)

29) G. S. Manning, *J. Chem. Phys.* **51**, 924, 934, 3249 (1969)

30) G. S. Manning, *Ann Rev. Phys. Chem.* **23**, 117 (1972)

31) R. M. Fuoss, A. Katchalsky, S. Lifson, *Proc. Natl. Acad. Sci. U.S.A.* **37**, 579 (1951)

32) T. Alfrey, P. W. Berg, H. Morawetz, *J. Polym. Sci.* **7**, 543 (1951)

33) J.Blaul, M. Ballauff, in preparation

34) For the possible reasons of this failure of the cell model, see P. S. Kuhn, Y. Levin, M. C. Barbosa, *Macromolecules* **31**, 8347 (1998)

35) M. Rehahn, *Acta Polymerica* **49**, 201 (1998)

36) F. Ciardelli, E. Tsuchida, D. Wöhrle, *Macromolecule-Metal-Complexes*, Springer, Berlin, 1996

37) V. Balzani, A. Juris, M. Venturi, S. Campagna, S. Serroni, *Chem. Rev.* **96**, 759 (1996)

38) A. Harriman, R. Ziessel, *J. Chem. Soc., Chem. Commun.* 1707 (1996)

39) J.-M. Lehn, *Supramolecular Chemistry*, VCH, Weinheim, 1995

40) E. C. Constable, A. M. W. Chargill Thompson, *J. Chem. Soc., Dalton Trans.* 1615 (1995)

41) E. C. Constable, A. M. W. Cargill Thompson, P. Harveson, L. Macko, M. Zehnder, *Chem. Eur. J.* **1**, 360 (1995)

42) J.-P. Sauvage, J.-P. Collin, J.-C. Chambron, S. Guillerez, C. Coudret, V. Balzani, F. Barigelletti, L. DeCola, L. Flamigni, *Chem. Rev.* **94**, 993 (1994)

43) R. Knapp, A. Schott, M. Rehahn, *Macromolecules* **29**, 478 (1996)

44) S. Kelch, M. Rehahn, *Macromolecules* **30**, 6185 (1997)

45) S. Kelch, M. Rehahn, *Macromolecules* **31**, 4102 (1998)

46) S. Kelch, M. Rehahn, manuscript submitted

47) M. Beley, S. Chodorowski, J.-P. Collin, J.-P. Sauvage, L. Flamigni, F. Barigelletti, *Inorg. Chem.* **33**, 2543 (1994)

48) W. Spahni, G. Calcaferri, *Helv. Chim. Acta* **67**, 450 (1984)

49) M. Rehahn, A.-D. Schlüter, G. Wegner, *Makromol. Chem.* **191**, 1991 (1990)

50) L. Schmitz, M. Ballauff, *Polymer* **36**, 879 (1995)